

Simulations of Nano-Particle Electro-Luminescence for Novel Near-Field Microscopy

Syed Saad Ahsan

Applied and Engineering Physics, Cornell University

NNIN REU Site: Microelectronics Research Center, The University of Texas at Austin

NNIN REU Principal Investigator: Dr. John X.J. Zhang, Biomedical Engineering, The University of Texas at Austin

NNIN REU Mentors: Ashwini Gopal and Kazunori Hoshino, Biomedical Engineering, The University of Texas at Austin

Contact: ssa27@cornell.edu, John.Zhang@engr.utexas.edu

Abstract

We simulated two-dimensional electro-luminescence (EL) performances of organic multi-layered quantum dot light emitting diodes (QD-LEDs), through iterative time-step calculations. Simulations were run for LED anode-cathode pairs of various overlapping length. Our simulation results showed that: (1) nearly all recombination happened on the QD mono-layer; (2) when the spatial overlap was zero, the area of emission could be further decreased to 50 nm under driving current densities at the mA/cm² level; and (3) with increasing driving current, the decay time of the excitons significantly slow down leading to the saturation of neighboring QDs, and therefore loss in resolution.

Introduction

The resolution of near-field optical signals, captured at a distance shorter than the wavelength of the emitted light, is determined by area of light emission rather than Rayleigh diffraction. Near-field scanning optical microscopes (NSOMs) use this phenomenon on scanning probe microscopes (SPM). Light emitting diodes (LEDs) can be incorporated on the probe tip leading to aperture free NSOMs [1]. We have fabricated a silicon microprobe integrated with a nanometer-sized LED, consisting of organic quantum dots (QD) on the tip, for NSOM. The physical properties of the QD-LED directly define the spectral range and imaging resolution due to the quantum confinement effects.

Methodology

We applied the Poisson equation using the charge distribution to solve the potential which was consequently used to determine charge transport. We then ran a time-step process until steady-state solution was achieved. Quantum tunneling is assumed over nanocrystal energy barriers.

Device Schematic (refer to Figure 1)

The LED was designed to have ohmic electrode contacts, organic transport layers and a monolayer of capped nano-particles. Our two-dimensional simulations varied the lengths of the spatial overlap between the two electrodes. All simulations were done in MATLAB[®].

Algorithm Outline

The algorithm basically divided our LED device into many subdivisions. Each subdivision being 10 nm wide and 2 nm tall, which was consequently the resolution of our two-dimensional solution. To decrease run time, we found the smallest device width after which the position-dependent variable distributions

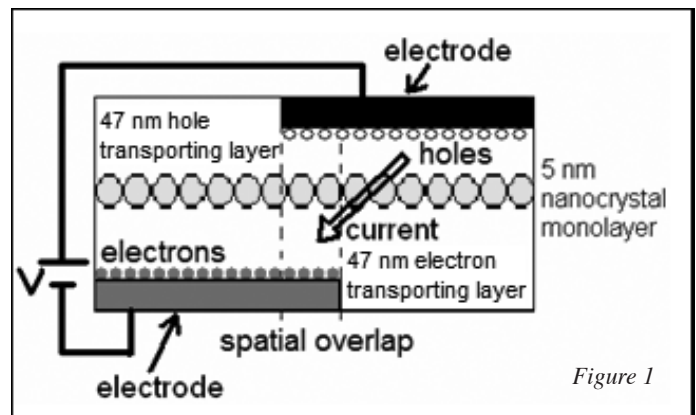


Figure 1

did not change significantly. For no spatial overlap, our device was 500 nm.

We assumed several variables that were functions of position such as potential, electric field, and carrier transport. Each iteration solved the potential using the charge distribution, and found the new charge distribution from finding charge transport determined from potential. We ran these iterations until the steady state condition [3] was reached:

$$\nabla J_n/q = -\nabla J_p/q = Bnp \quad (\text{Recombination}) \quad (1)$$

where the divergence of the current densities over the charge of the carriers, q , was equal to the recombination that occurred at each division. The Langevin recombination constant B was equal to $10^{-18} \text{m}^3/\text{sec}$.

Potential

The potential was determined using the charge distribution by solving the Poisson equation [2]:

$$\nabla^2 \Phi = q(p-n)/\epsilon \quad (2)$$

where ϵ represents the permittivity of free space, p and n represent the hole and electron carrier concentrations and Φ represents the potential. After defining relevant boundary conditions, we numerically solved the potential employing matrices.

Charge Transport

Assuming that carrier injection was due to thermionic emission at the ohmic electrodes, the carrier density at the electrodes was approximated [3] as $10^{24}/\text{m}^3$ for holes at the cathode and the electrons at the anode.

We assumed that the charge transport [2] was composed of drift and diffusion:

$$J_p = q(\mu_p p E + D_p \nabla p) \quad (3)$$

$$J_n = q(\mu_n n E + D_n \nabla n) \quad (4)$$

where μ represents the mobility variable, D represents the diffusion variable and E represents the electric field. Mobility and diffusion were also functions of position being dependent on electric field [2] as in an electron-hopping like model:

$$\mu_{n/p} = \mu_{0\ n/p} \sqrt{(E/E_{pf})} \quad (5)$$

$$D = \mu KT/q \quad (6)$$

where $\mu_{0\ n/p}$ is the mobility constant, and E_{pf} is the activation field related to disorder equal to 10^7 V/m. The mobility constant for each carrier at its respective transport layer was 10^{-10} m^2/Vs and in the other layer as 10^{-12} m^2/Vs [3]. Treating our equations like vectors, we calculated each dimensional component.

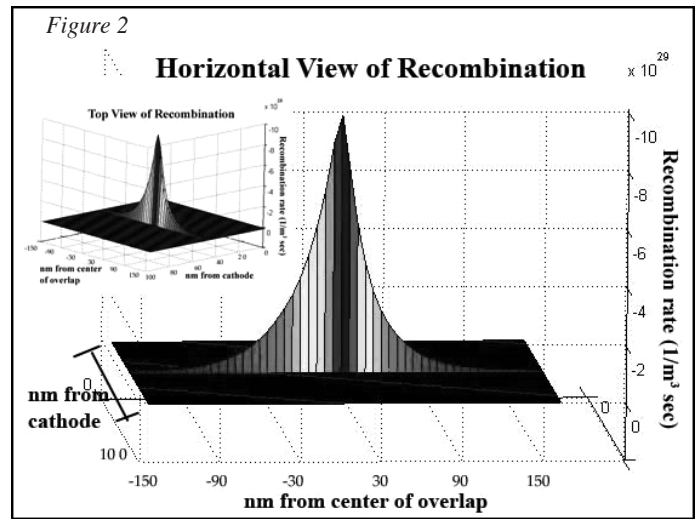
Across the nanocrystal monolayer, we found charge flow by taking quantum transmission rates over square wells or barriers using one-dimensional Boltzmann-Maxwellian velocity distributions. The energy diagram was found in previous literature [4] assuming that the transporting layers were PBD, TPD, and the nanocrystals were CdSe.

Exciton Kinetics

We assumed that light originated from Forster energy transfers into the nanocrystal monolayer with a slow diffusion limit [5]. We only considered the excitons formed in the nanocrystal monolayer presuming that most of the excitons would form in the monolayer. Because the diffusion coefficient is inversely related to the decay rate squared, τ_{exc}^{-2} , we assumed a modestly long τ_{exc} of 100 ns which would correspond to relatively slow exciton diffusion for CdSe nanocrystals.

Results And Discussion

The recombination profile (see Figure 2) shows that exciton formation occurs only on the nanocrystal monolayer. We expect that since the monolayer is also the most radiative part of the device, the light emission should be easily confined to these nanocrystals. This also verifies our initial assumptions that only the excitons formed on the monolayer are important in computing Forester energy transfers.



Additionally when spatial overlap is zero (see Figure 3), the area of light emission is further confined to 50 nm inside the monolayer at low voltages.

At higher driving currents, the low exciton limit [5], where the exciton injection rate $< \tau_{exc}^{-1}$, is not fulfilled anymore as nanocrystals get more than one exciton (see Figure 4), produced biexcitons and led to slower decay rates. When this happened, there was a loss of resolution implying that the tradeoff for low exciton diffusion was lower light intensities.

Acknowledgements

I would like to acknowledge the National Science Foundation, the National Nanotechnology Infrastructure Network Research Experience for Undergraduates Program, and Dr. Sanjay Banerjee for the support. I would also like to thank the Zhang research lab and especially God.

References

- [1] K. Hoshino et al., MEMS, p.743 (2007).
- [2] S. Chang et al., Proc. SPIE, p. 26-1 (2006).
- [3] B. Crone et al., J. Appl. Phys., p.833 (1998).
- [4] Zhao et. al., J. Appl. Phys., p.3207 (2004).
- [5] K. Kohary et. Al., J. Appl. Phys., 114315 (2006).

